Inorg. Chem. **2009**, *48*, 2865−2872

Inorganic Chemistry
Article

Magnetostructural Correlations in $Cu^{II}-NC-W^{V}$ Linkage: The Case of $[Cu^{II}(diimine)]^{2+}-[W^{V}(CN)_8]^{3-}$ 0D Assemblies

Tomasz Korzeniak,[*,†] Cédric Desplanches,[‡] Robert Podgajny,[†] Carlos Giménez-Saiz,[§]
Katarzyna Stadnicka,[†] Michał Rams,[||] and Barbara Sieklucka[†]

Faculty of Chemistry, Jagiellonian University, Ingardena 3, 30-060 Kraków, Poland, Université Bordeaux 1, CNRS, Institut de Chimie de la Matière Condensée de Bordeaux, UPR9048, 87 avenue du Dr. A. Schweitzer, 33608 Pessac Cedex, France, Institute for Material Science, University of Valencia, Polígon La Coma, 46980 Paterna, Spain, and M. Smoluchowski Institute of Physics, Jagiellonian University, Reymonta 4, 30-059 Kraków, Poland

Received October 17, 2008

We report on the syntheses, crystal structures, and magnetic properties of two cyano-bridged molecular assemblies: $[Cu^{II}(phen)_3]_2\{[Cu^{II}(phen)_2]_2[W^{V}(CN)_8]_2\}(ClO_4)_2 \cdot 10H_2O$ (phen = 1,10-phenanthroline) (**1**) and $\{[Cu^{II}(bpy)_2]_2[W^{V}(CN)_8]\}\{[Cu^{II}(bpy)_2][W^{V}(CN)_8]\} \cdot 4H_2O$ (bpy = 2,2′-bipyridyl) (**2**). Compound **1** consists of cyano-bridged $[Cu^{II}{}_2W^{V}{}_2]^{2-}$ molecular rectangles and isolated $[Cu^{II}(phen)_3]^{2+}$ complexes. The molecular structure of **2** reveals cyano-bridged trinuclear $[Cu^{II}{}_2W^{V}]^{+}$ and dinuclear $[Cu^{II}W^{V}]^{-}$ ions. Magnetic interactions in **1** are interpreted in terms of the model of a tetranuclear moiety consisting of two ferromagnetic $Cu^{II}-NC-W^{V}$ units ($J_1 = +39(4)$ cm^{-1}) interacting antiferromagnetically ($J_2 = -1.6(4)$ cm^{-1}). The analysis of the magnetic response of **2** reveals ferromagnetic interaction within the $[Cu^{II}-NC-W^{V}-CN-Cu^{II}]^{+}$ and $[Cu^{II}-NC-W^{V}]^{-}$ isolated units, characterized by $J = +35(7)$ cm^{-1} and antiferromagnetic coupling between them ($4J' = -0.30(8)$ cm^{-1}). The discussion of the magnetic behavior and the correlation of the J_{CuW} parameters with the geometry of cyano bridges at copper(II) centers of **1** and **2** is based on the DFT calculations, which yield $J_{av} = +13.2$ cm^{-1} for **1** and $J = +31$ cm^{-1} for **2**. The domination of the ferromagnetic $Cu^{II}-NC-W^{V}$ interaction in **1** and **2** originates from the mutual orthogonality of natural magnetic orbitals in the case of coordination of cyano bridges at the equatorial sites of Cu(II) moieties.

Introduction

Molecular magnetic materials built of paramagnetic 3d or 4f metal centers linked by octacyanometalate units are clearly recognized as potential functional materials.[1−28] In this context, cyano-bridged Cu(II)−octacyanometalate(V,IV) (M = Mo, W) assemblies are among the most extensively studied systems.[9−28] The dynamic research activity in this field resulted in construction of the heterobimetallic clusters and extended networks. The majority of cyano-bridged $Cu^{II}-NC-W^{V}$ systems display dominant ferromagnetic coupling between metal centers, which is usually accompanied by much weaker intra- or intermolecular antiferromagnetic coupling,[10−21] leading to metamagnetism in some cases.[10−13] The magnetic coupling constants for the *local* $M^{V}-CN-Cu^{II}$ arrangements were estimated *only* for limited examples of 1D and 2D cyano-bridged architectures.[17−20] The results indicate that the nature and the magnitude of magnetic interaction may strongly depend on the coordination number, geometry, and positions of cyano bridges at the coordination sphere of the Cu(II) center. This dependence is particularly pronounced for the two cases where the $Cu^{II}-N_{CN}$ distances obey the classical coordination bonding limit of 2.3 Å for copper(II) complexes. The value of $J_{WCu} = +5.8$ cm^{-1} calculated for the dinuclear motif $[Cu^{II}(tren)][W^{V}(CN)_8]^{-}$ in the 2D $[Cu^{II}(tren)]\{Cu^{I}[W^{V}$-

---

[*] To whom correspondence should be addressed. E-mail: korzenia@chemia.uj.edu.pl.

[†] Faculty of Chemistry, Jagiellonian University.

[‡] Université Bordeaux 1.

[§] University of Valencia.

[||] M. Smoluchowski Institute of Physics, Jagiellonian University.

(1) Przychodzeń, P.; Korzeniak, T.; Podgajny, R.; Sieklucka, B. *Coord. Chem. Rev.* **2006**, *250*, 2234–2260.

(2) Catala, L.; Mathonière, C.; Gloter, A.; Stephan, O.; Gacoin, Th.; Boilot, J. P.; Mallah, T. *Chem. Commun.* **2005**, 746−748.

(3) Ohkoshi, S.; Ikeda, S.; Hozumi, T.; Kashigawi, T.; Hashimoto, K. *J. Am. Chem. Soc.* **2006**, *128*, 5320–5321.

(4) Wang, Z.; Li, X.; Wang, T.; Li, Y.; Ohkoshi, S.; Hashimoto, K.; Song, Y.; You, X. *Inorg. Chem.* **2007**, *46*, 10990. Zhao, H.; Shatruk, M.; Prosvirin, A. V.; Dunbar, K. R. *Chem.—Eur. J.* **2007**, *13*, 6573–6589.

10.1021/ic801989b CCC: $40.75

$(CN)_8]\}\cdot 1.5H_2O$[19] assembly is evidently lower than the $J_{WCu} = +35$ cm^{-1} estimated for pentameric $Cu^{II}_3W^V_2$units in the 2D $\{Cu^{II}_3(\mu{-}4,4'\text{-bpy})_3DMF_6\ [W^V(CN)_8]_2\}\cdot 2H_2O$[20] network. In the molecular structure of $[Cu^{II}(tren)]\{Cu^I[W^V(CN)_8]\}\cdot 1.5H_2O$, the single cyano bridge is located at the axial position in the trigonal bipyramidal (TBPY-5) coordination sphere of Cu(II), whereas in the case of $\{Cu^{II}_3(\mu{-}4,4'\text{-bpy})_3DMF_6[W^V(CN)_8]_2\}\cdot 2H_2O$, the two cyano bridging ligands are situated at the equatorial positions of the elongated octahedral Cu(II) coordination environment. This implies the nonequivalency of the copper(II) magnetic orbitals involved in the exchange pathways, with short $Cu-N_{NC}$ distances (~2.00 Å) in both cases and different Cu−NC bending angles (160° for the $Cu^{II}Cu^IW^V$ system vs 151° and 171° for $Cu^{II}_3W^V_2$). Taking into account these factors, it is important to validate the influence of the $Cu^{II}-NC-W^V$ linkage geometry and the coordination polyhedra of metal centers on the nature and the magnitude of magnetic coupling. Analysis of the magnetic properties of discrete molecules with well-defined Cu(II) and octacyanometalate(V) coordination geometry, reducing inaccuracy in J_{WCu} assessment, could lead to the accomplishment of magnetostructural correlations.

To construct the molecular compounds with $Cu^{II}-NC-W^V$ linkages, we have chosen $[Cu^{II}(bpy)_2]^{2+}$ and $[Cu^{II}(phen)_2]^{2+}$ building blocks, which allow the formation of low-dimensional systems due to substitution of the labile aqua ligands. We were inspired by the trinuclear molecule $[Cu^{II}(bpy)_2]_2[Mo^{IV}(CN)_8]\cdot 5H_2O\cdot CH_3OH$ with single cyano bridges at equatorial positions of the trigonal bipyramidal Cu(II) centers.[22] This molecule reveals the transition to the photoinduced antiferromagnetic state $Cu^{II}Mo^VCu^{II}$. Herein, we report on the syntheses, X-ray crystal structures, and magnetic properties of the two novel molecular cyano-bridged assemblies $[Cu^{II}(phen)_3]_2\{[Cu^{II}(phen)_2]_2[W^V(CN)_8]_2\}(ClO_4)_2\cdot 10H_2O$ (**1**) and $\{[Cu^{II}(bpy)_2]_2[W^V(CN)_8]\}\{[Cu^{II}(bpy)_2][W^V(CN)_8]\}\cdot 4H_2O$ (**2**). The molecular structure of **1** consists of $[Cu^{II}_2W^V_2]^{2-}$ molecular rectangles and isolated $[Cu^{II}(phen)_3]^{2+}$ complexes, in structural resemblance to the $Mn^{II}_2W^V_2$ molecular squares present in $[Mn(tptz)\ (CH_3COO)(H_2O)_2]_2\{[Mn(tptz)(CH_3OH)_{1.58}(H_2O)_{0.42}]_2[W(CN)_8]_2\}\cdot 5CH_3OH\cdot 9.85H_2O$ (tptz = 2,4,6-tris(2-pyridyl)- 1,3,5-triazine) and $\{Mn^{II}(bpy)_2]_2(ox)\}\{[Mn^{II}(bpy)_2W(CN)_8]_2\}\cdot 4H_2O$ (ox = oxalate).[4] The molecular structure of **2** reveals the presence of dinuclear $[Cu^{II}W^V]^-$ and almost linear trinuclear $[Cu^{II}_2W^V]^+$ units. The analogous nuclearity exhibits ferromagnetic $[CuL]_3[W(CN)_8]_2\cdot 4H_2O$, (L = 3,7-bis(2-aminoethyl)-1,3,5,7-tetraazabicyclo[3.3.2]decane), although the trinuclear Cu_2W unit shows a Cu−W−Cu angle close to 90°.[24] The discussion of the magnetic behavior and the correlation of the J_{CuW} parameters with the geometry of cyano bridges at copper(II) centers of **1** and **2** is based on DFT calculations.

Experimental Section

Materials. 1,10-Phenanthroline and 2,2′-bipyridyl were purchased from commercial sources (Aldrich) and used as received. Octacyanotungstate(V) sodium[29] and cesium[30] salts have been synthesized according to the published procedures. **Caution!** *Perchlorate salts of transition metals are potentially explosive and, therefore, should be used in small amounts and handled with care!*

Synthesis of $[Cu^{II}(phen)_3]_2[Cu^{II}(phen)_2(\mu\text{-}NC)_2W^V(CN)_6]_2(ClO_4)_2\cdot 10H_2O$ (1). To a stirred solution of 1,10-phenanthroline (0.476 g, 2.4 mmol, 30 mL of H_2O/CH_3CN, 1:1 v/v) was added a solution of $Cu(ClO_4)_2\cdot 6H_2O$ (0.315 g, 0.85 mmol, 60 mL of H_2O:CH_3CN, 1:1 v/v), followed by the addition of $Cs_3[W^V(CN)_8]\cdot 2H_2O$ (0.38 g, 0.46 mmol) dissolved in 60 mL of H_2O/CH_3CN, 1:1 v/v. The solution was allowed to evaporate for 10 days, then it was filtered. Green crystals were formed after 2 weeks. Yield: 80 mg, 12%. Elem anal. for $C_{136}H_{96}W_2Cu_4Cl_2O_{16}N_{36}$ (**1** − $2H_2O$): C, 51.31; N, 15.84 H, 3.04. Found: C, 51.12; N, 16.37; H, 3.15. IR spectrum

---

(5) Withers, J. R.; Li, D.; Triplet, J.; Ruschman, Ch.; Parkin, S.; Wang, G.; Yee, G. T.; Holmes, S. *Inorg. Chem.* **2006**, *45*, 4307–4309.

(6) Przychodzeń, P.; Pełka, R.; Lewiński, K.; Supel, J.; Rams, M.; Tomala, K.; Sieklucka, B. *Inorg. Chem.* **2007**, *46*, 8924–8938.

(7) Nowicka, B.; Rams, M.; Stadnicka, K.; Sieklucka, B. *Inorg. Chem.* **2007**, *46*, 8123–8125.

(8) Lim, J. H.; Yoon, J. H.; Kim, H. Ch.; Hong, Ch. S. *Angew. Chem., Int. Ed.* **2006**, *45*, 7424–7426.

(9) Ohkoshi, S.; Tokoro, H.; Hozumi, T.; Zhang, Y.; Hasimoto, K.; Mathonière, C.; Bord, I.; Rombaut, G.; Verelst, M.; Cartier dit Moulin, Ch.; Villain, F. *J. Am. Chem. Soc.* **2006**, *128*, 270–277. Zhang, Y.; Hozumi, T.; Hashimoto, K.; Ohkoshi, S. *Acta Crystallogr., Sect. E* **2007**, *63*, i30–i32.

(10) Ohkoshi, S.; Arimoto, Y.; Hozumi, T.; Seino, H.; Mizobe, Y.; Hashimoto, K. *Chem. Commun.* **2003**, 2772−2773.

(11) Li, D.; Zheng, L.; Wang, X.; Huang, J.; Gao, S.; Tang, W. *Chem. Mater.* **2003**, *15*, 2094–2098.

(12) Podgajny, R.; Korzeniak, T.; Bałanda, M.; Wasiutyński, T.; Errington, W.; Kemp, T. J.; Alcock, N. W.; Sieklucka, B. *Chem. Commun.* **2002**, 1138–1139. Korzeniak, T.; Podgajny, R.; Alcock, N. W.; Lewiński, K.; Bałanda, M.; Wasiutyński, T.; Sieklucka, B. *Polyhedron* **2003**, *22*, 2183–2190. Sieklucka, B.; Korzeniak, T.; Podgajny, R.; Bałanda, M.; Nukazawa, Y.; Myiazaki, Y.; Sorai, M.; Wasiutyński, T. *J. Magn. Magn. Mater.* **2004**, *272−276*, 1058–1059. Bałanda, M.; Korzeniak, T.; Pełka, R.; Podgajny, R.; Rams, M.; Sieklucka, B.; Wasiutyński, T. *Solid State Sci.* **2005**, *7*, 1113–1124.

(13) Podgajny, R.; Chmel, N. P.; Bałanda, M.; Tracz, P.; Gaweł, B.; Zając, D.; Sikora, M.; Kapusta, C.; Łasocha, W.; Wasiutyński, T.; Sieklucka, B. *J. Mater. Chem.* **2007**, *17*, 3308–3314.

(14) Ohkoshi, S.; Tsunobuchi, Y.; Takahashi, H.; Hozumi, T.; Shiro, M.; Hashimoto, K. *J. Am. Chem. Soc.* **2007**, *129*, 3084–3085.

(15) You, S. Y.; Yoon, J. H.; Lim, J. H.; Kim, H. Ch.; Hong, Ch. S. *Inorg. Chem.* **2005**, *44*, 7063–7069.

(16) Lim, J. H.; Kang, J. S. ; Kim, H. Ch.; Koh, E. K.; Hong, Ch. S. *Inorg. Chem.* **2006**, *45*, 7821–7827.

(17) Li, D.; Gao, S.; Zheng, L.; Yu, K.; Tang, W. *New. J. Chem.* **2002**, *26*, 1190–1195.

(18) You, Y. S.; Kim, D.; Do, Y.; Oh, S. J.; Hong, Ch. S. *Inorg. Chem.* **2004**, *43*, 6899–6901.

(19) Korzeniak, T.; Stadnicka, K.; Bałanda, M.; Tomala, K.; Kowalski, K.; Sieklucka, B. *Chem. Commun.* **2005**, 2939−2941.

(20) Korzeniak, T.; Stadnicka, K.; Rams, M.; Sieklucka, B. *Inorg. Chem.* **2004**, *43*, 4811–4813.

(21) Li, D.; Gao, S.; Zheng, L.; Sun, W.; Okamura, T.; Ueyama, N.; Tang, W. *New J. Chem.* **2002**, *26*, 485–489.

(22) Rombaut, G.; Verelst, M.; Gohlen, S.; Ouahab, L.; Mathoniere, C.; Kahn, O. *Inorg. Chem.* **2001**, *40*, 1151–1159.

(23) Herrera, J. M.; Marvaud, V.; Verdaguer, M.; Marrot, J.; Kalisz, M.; Mathoniere, C. *Angew. Chem., Int. Ed.* **2004**, *43*, 5468–5471.

(24) Kou, H.; Zhou, B.; Si, S.; Wang, R. *Eur. J. Inorg. Chem.* **2004**, 401−408.

(25) Hozumi, T.; Hashimoto, K.; Ohkoshi, S. *J. Am. Chem. Soc.* **2005**, *127*, 3864–3869.

(26) Wang, Zh. X.; Zhang, P.; Shen, X. F.; Song, Y.; You, X. Z.; Hashimoto, K. *Cryst. Growth Des.* **2006**, *6*, 2457–2462.

(27) Hozumi, T.; Nuida, T.; Hashimoto, K.; Ohkoshi, S. *Cryst. Growth Des.* **2006**, *6*, 1736–1737.

(28) Lim, J. H.; Kang, J. S.; Kim, H. Ch.; Koh, E. K.; Hong, Ch. S. *Inorg. Chem.* **2006**, *45*, 7821–7827. Lim, J. H.; You, Y. S.; Yoo, H. S.; Yoon, J. H.; Kim, J. I.; Koh, E. K.; Hong, Ch. S. *Inorg. Chem.* **2007**, *46*, 10578–10586.

(29) Samotus, A. *Pol. J. Chem.* **1973**, *47*, 653.

(30) Bok, L. D. C.; Leipoldt, J. G.; Basson, S. S. *Z. Anorg. Allg. Chem.* **1975**, *415*, 81–83.

Table 1. Crystal Data for **1** and **2**

	1	**2**
empirical formula	$C_{136}H_{100}Cl_2Cu_4N_{36}O_{18}W_2$	$C_{76}H_{58}Cu_3N_{28}O_5W_2$
fw	3219.28	2001.82
temperature	292(2) K	293(2) K
wavelength	0.71069 Å	0.71073 Å
crystal system	monoclinic	orthorhombic
space group	*P*21/*c*	*P*212121
unit cell dimensions	$a = 12.1598(2)$ Å	$a = 14.9154(1)$ Å
	$b = 33.8796(4)$ Å	$b = 20.1800(1)$ Å
	$c = 18.8642(2)$ Å	$c = 30.0374(2)$ Å
volume	6708.82(15) $Å^3$	9041.04(10) $Å^3$
Z	2	4
density (calculated)	1.594 Mg/m^3	1.471 Mg/m^3
abs coeff	2.450 mm^{-1}	3.290 mm^{-1}
F(000)	3220	3940
cryst size	$0.20 \times 0.10 \times 0.10$ mm^3	$0.42 \times 0.37 \times 0.20$ mm^3
θ range for data collection	2.19−27.61°	2.910−32.032°
index ranges	$-15 \leq h \leq 15$	$0 \leq h \leq 20$
	$-44 \leq k \leq 44$	$0 \leq k \leq 27$
	$-24 \leq l \leq 24$	$-39 \leq l \leq 39$
reflns collected	30465	23238
independent reflns	15427 [R(int) = 0.0453]	23238 [R(int) = 0.0000]
completeness to θ	99.0% ($\theta = 27.61°$)	89.7% ($\theta = 30.25°$)
abs correction	none	multiscan
refinement method	full-matrix least-squares on F^2	full-matrix least-squares on F^2
data/restraints/params	15427/50/927	23238/0/997
goodness-of-fit on F^2	1.025	1.064
final R indices [$I > 2\sigma(I)$]	R1 = 0.0436, wR2 = 0.1024	R1 = 0.0612, wR2 = 0.1199
R indices (all data)	R1 = 0.0821, wR2 = 0.1154	R1 = 0.1196, wR2 = 0.1420
largest diff. peak and hole	0.767 and −0.695 e $Å^{-3}$	0.980 and −0.611 e A^{-3}

in ν(CN) region: 2139m, 2190m is consistent with the presence of $W^{V}-CN-Cu^{II}$ and $W^{V}-CN$ coordination arrangements.

Synthesis of $\{[Cu^{II}(bpy)_2]_2[W^{V}(CN)_8]\}\{[Cu^{II}(bpy)_2][W^{V}(CN)_8]\}\cdot 4H_2O$ (2). The crystals were grown by a slow diffusion of aqueous solutions of $Cu(NO_3)_2\cdot 3H_2O$ (0.05 g, 0.21 mmol) and $Na_3[W^{V}(CN)_8]\cdot 1.5H_2O$ (0.10 g, 0.19 mmol) through a solution of 2,2′-bpy (0.20 g, 1.28 mmol, H_2O:C_2H_5OH, 1:1 v/v) in H tubes. Green needle-shaped crystals were formed within two months. Yield: 53 mg, 38%. Elem anal. for $C_{76}H_{58}W_2Cu_3O_5N_{28}$: C, 45.60; N, 19.59; H, 2.92. Found: C, 45.39; N, 19.20; H, 2.76. IR spectrum in ν(CN) region: 2114sh, 2142m, 2150sh, 2176m is consistent with the presence of $W^{V}-CN-Cu^{II}$ and $W^{V}-CN$ coordination arrangements.

X-Ray Crystallographic Data Collection and Refinement of the Structures. The crystal structures of **1** and **2** were determined from the single-crystal X-ray diffraction data collected at 293(2) K with a Nonius KappaCCD diffractometer using a graphite-monochromated Mo Kα radiation source ($\lambda = 0.71073$ Å). The DENZO and SCALEPACK[31] programs were used for cell refinements and data reduction. No absorption corrections were performed for **1**. Absorption corrections were introduced for **2** using the Multiscan method.[31] The structures were solved by direct methods using the SIR92[32] program with the WinGX[33] graphical user interface. The structure refinements were carried out with SHELXL-97.[34]

In the case of **1**, the oxygen atoms of the perchlorate anion are disordered between two different positions with refined partial occupancies of 0.6633 and 0.3367. Seven crystallographically independent water molecules were found in the structure; of those, O1W, O2W, and O3W have occupancies of 1.0, while O4W, O5W, O6W, and O7W have occupancies of 0.5, giving a total of 10 water molecules in the formula unit. The oxygen atoms with partial occupancies were not refined anisotropically. All other non-hydrogen atoms were refined anisotropically. The hydrogen atoms on carbon atoms were included at calculated positions and refined with a riding model. Hydrogen atoms of water molecules were not located. Complete crystallographic data and data collection parameters are summarized in Table 1.

In **2**, all non-hydrogen atoms were refined anisotropically, except oxygen atoms corresponding to water molecules which were refined isotropically. The O1W−O6W atoms have occupancies of 0.98, 0.90, 0.62, 0.66, 0.38, and 0.46, respectively, whereas O7W−O10W have occupancies of 0.25 each, giving a total of five water molecules in the formula unit. Hydrogen atoms of aromatic CH were included at calculated positions and refined in a riding model with parameters 1.2× those for parent atoms. Hydrogen atoms of water molecules were not located on difference Fourier maps.

Computational Methodology. Standard DFT calculations have been previously used for the evaluation of exchange coupling constants for transition metal dimers, including some of the second-row transition series.[35−38] For each coupling constant, two separate DFT calculations were carried out, one for the highest spin state (i.e., triplet, quadruplet, and quintet states for the dimeric, trimeric, and tetrameric species considered here, respectively) and one for

---

(31) Otwinowski Z.; Minor, W. DENZO-SCALEPACK, Processing of X-ray Diffraction Data Collected in Oscillation Mode. In *Methods Enzymol.*; Carter, C. W., Jr., Sweet, R. M., Eds.; Academic Press: New York, 1997; Macromolecular Crystallography, Part A, Vol. *276*.

(32) Altomare, A.; Burla, M. C.; Camalli, M.; Cascarano, G.; Giacovazzo, C.; Guagliardi, A.; Moliterni, A. G. G.; Polidori, G.; Spagna, R. *J. Appl. Crystallogr.* **1999**, *32*, 115–119.

(33) Farrugia, L. J. *J. Appl. Crystallogr.* **1997**, *32*, 837.

(34) Sheldrick, G. M. *SHELXL-97*; University of Goettingen: Goettingen, Germany, 1997.

(35) Ruiz, E.; Rajaraman, G.; Alvarez, S.; Gillon, B.; Stride, J.; Clerac, R.; Larionova, J.; Decurtins, S. *Angew. Chem., Int. Ed.* **2005**, *44*, 2711–2715.

(36) Desplanches, C.; Ruiz, E.; Alvarez, S. *Eur. J. Inorg. Chem.* **2003**, 1756–1760.

(37) Low, D. M.; Rajaraman, G.; Helliwell, M.; Timco, G.; van Slageren, J.; Sessoli, R.; Ochsenbein, S. T.; Bircher, R.; Dobe, Ch.; Waldmann, O.; Gudel, H.; Adams, M. A.; Ruiz, E.; Alvarez, S.; McInnes, E. *Chem.—Eur. J.* **2006**, *12*, 1385–1396.

(38) Ruiz, E.; Nunzi, F.; Alvarez, S. *Nano Lett.* **2006**, *6*, 380–384.

the broken-symmetry state. The hybrid B3LYP[39] functional was used as implemented in Gaussian98.[40] The bases used in all calculations were the D95 Dunning−Huzinaga valence double-ζ[41] for first-row elements and the small-core Hay−Wadt pseudopotential[42] for transition metals (indicated in the Gaussian code as LANL2DZ). For the dinuclear species, the J values were then obtained by considering $E_{HS} - E_{BS} = -J(2S_1S_2 + S_2) = -J$, where S_1 and S_2 are the spins of the two metal centers ($S_1 = S_2 = 1/2$) and E_{HS} and E_{BS} are the energies of the high-spin and broken-symmetry states, respectively. We assumed that the energy of the broken-symmetry state is a good approximation of low-spin state energy, following Ruiz et al.[43,44] For the trinuclear and tetranuclear units, the procedure developed by Ruiz et al. has been used.[45] Spin population analyses were carried out with the Gaussian code in the NBO framework.[46] The natural orbitals represented here were computed with Gaussian98.[47]

Physical Techniques. Infrared spectra were recorded on Bio-Rad FTS 165 FT-IR and Bruker EQUINOX 55 FT-IR spectrometers. Elemental analyses were performed on a EuroVector EuroEA instrument. Magnetic measurements were performed using a Quantum Design MPMS5-XL magnetometer. Samples were prepared in the form of pellets to avoid magnetic signals from a container. The core diamagnetism of the samples was carefully substracted.[48]

Results and Discussion

Crystal Structures. The crystal structure of $[Cu^{II}(phen)_3]_2\{[Cu^{II}(phen)_2]_2[W^{V}(CN)_8]_2\}(ClO_4)_2\cdot 10H_2O$ (**1**) consists of the tetrametallic rectangles $\{[Cu^{II}(phen)_2(\mu\text{-}NC)_2W^{V}(CN)_6]_2\}^{2-}$, $[Cu(phen)_3]^{2+}$ cations, ClO_4^- anions, and crystallization water molecules (Figure 1). The selected bond lengths and angles are presented in Table 2. The octacyanotungstate(V) ion reveals distorted bicapped trigonal prism (BTP-8) geometry, with slightly marked features of a square antiprism (SAPR-8), which was concluded from the values of the shape-determining angles—the dihedral ϕ angles (defined as deviation from planarity of the atoms forming a trapezoid) and δ angles (dihedral angles at shape-determining edges)[49] (Table S1, Figure S1, Supporting Information)—along with the *continuous shape measures* (CShM) analysis (Table S2, Supporting Information), which is a convenient method of probing the local geometry of metal centers.[50−54] Each octacyanotungstate ion forms two cyano bridges toward two Cu1 centers. The $[Cu1(phen)_2(NC)_2]$ unit adopts an elongated octahedral geometry, due to the Jahn−Teller effect. The equatorial positions are occupied by three N donors from phen ligands and one N end of the C1−N1−Cu1 cyano bridge. The Cu1−N1−C1−W1 linkage at the equatorial position is short and almost linear (Cu1−N1 = 1.976 Å, C1−N1−Cu1 = 169.5(4)°, W1−Cu1 = 5.248 Å). The axial positions in the coordination sphere of Cu1 are occupied by two N atoms: the remaining N atom of the phen ligand ($Cu-N_{phen}$ = 2.302 Å) and a N atom of the longer and more bent Cu1−N5−C5−W1 linkage (Cu1−N5 = 2.597 Å, C5−N5−Cu1 = 154.73°, W1−Cu1 = 5.739 Å). The angles between cyano bridges centered at W1 and Cu1 corners, C1−W1−C5 of 82.81(18)° and N1−Cu1−N5 of 88.30°, are close to the right angle, which allows tetrametallic unit formation.

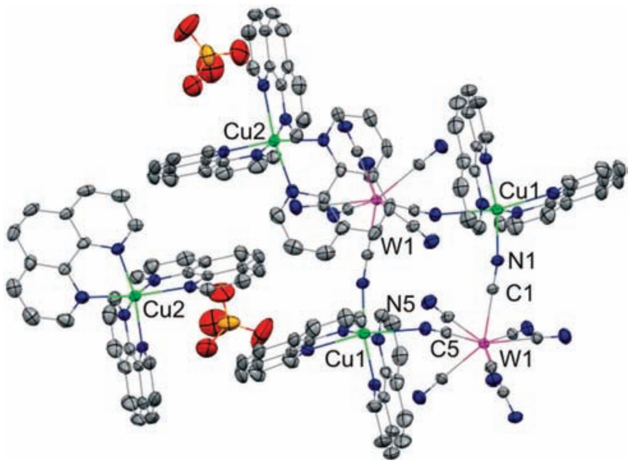

Figure 1. Molecular structure of **1** containing tetranuclear subunit with selected atoms labeling. Colors used: W, magenta; Cu, green; N, blue; C, gray; Cl, yellow; O, red. Water molecules have been removed for clarity. Thermal elipsoids of 25% probability are shown.

Table 2. Selected Bond Lengths [Å], Angles [deg], and Geometric Parameters of Cyano Bridges for **1**

Cu1−N1	1.976(4)	Cu2−N18	2.032(4)
Cu1−N5	2.597[a]	Cu2−N15	2.046(4)
Cu1−N9	2.023(4)	Cu2−N13	2.107(4)
Cu1−N10	2.042(4)	Cu2−N16	2.147(5)
Cu1−N12	2.045(4)	Cu2−N17	2.193(5)
Cu1−N11	2.302(4)	Cu2−N14	2.225(4)
Cu1−N1−C1	169.5(4)		
Cu1−N5−C5	154.73[a]	θ W1−C1	58.5
C1−W1−C5	82.81(18)	θ W1−C5	50.0
N1−Cu1−N5	88.3[a]		

[a] The metric parameters calculated with the use of the CCDC Mercury visualization software.

The Cu(II) centers located at the Cu2 crystallographic sites are surrounded by three phen ligands, giving the complex a distorted octahedral geometry. The equatorial coordination bonds reveal values slightly above 2 Å, contrary to much longer Cu−N bonds in the axial positions. The six-coordinative axially elongated $[Cu(phen)_3]^{2+}$ countercation is not very common in coordination chemistry; however, it is known to form stable ionic architectures together with simple

---

(39) Becke, A. D. J. *J. Chem. Phys.* **1993**, *98*, 5648–5652.
(40) Frisch, M. J. et al. *Gaussian98*; Gaussian, Inc.: Pittsburgh, PA, 1998.
(41) Dunning, T. H. J.; Hay, P. J. In *Modern Theoretical Chemistry*; Schaefer, H. F., III, Ed.; Plenum: New York, 1976; Vol. *3*.
(42) Hay, P. J.; Wadt, R. *J. Chem. Phys.* **1985**, *82*, 299–310.
(43) Ruiz, E.; Cano, J.; Alvarez, S.; Alemany, P. *J. Comput. Chem.* **1999**, *20*, 1391–1400.
(44) Ruiz, E.; Alvarez, S.; Cano, J.; Polo, V. *J. Chem. Phys.* **2005**, *123*, 164110.
(45) Ruiz, E.; Rodriguez-Fortea, A.; Cano, J.; Alvarez, S.; Alemany, P. *J. Comput. Chem.* **2003**, *24*, 982–989.
(46) Glendening, E. D.; Reed, A. E.; Carpenter, J. E.; Weinhold, F. *NBO 3.1*; University of Wisconsin: Madison, WI, 1996.
(47) Lowdin, P.-O. *Phys. Rev.* **1955**, *97*, 1474–1489.
(48) Kahn, O. *Molecular Magnetism*; VCH Publishers: New York, 1993.
(49) Muetterties, E. L.; Guggenberger, L. J. *J. Am. Chem. Soc.* **1974**, *96*, 1748–1756.
(50) Casanova, D.; Cirera, J.; Llunell, M.; Alemany, P.; Avnir, D.; Alvarez, S. *J. Am. Chem. Soc.* **2004**, *126*, 1755–1763.
(51) Alvarez, S.; Alemany, P.; Casanova, D.; Cirera, J.; Llunell, M.; Avnir, D. *Coord. Chem. Rev.* **2005**, *249*, 1693–1708.
(52) Casanova, D.; Llunell, M.; Alemany, P.; Alvarez, S. *Chem.—Eur. J.* **2005**, *11*, 1479–1494.
(53) Cirera, J.; Ruiz, E.; Alvarez, S. *Chem.—Eur. J.* **2006**, *12*, 3162–3167.
(54) Llunell, M.; Casanova, D.; Cirera, J.; Bofill, J. M.; Alemany, P.; Alvarez, S.; Pinsky, M.; Anvir, D. *SHAPE*, v. 1.1b.; University of Barcelona: Barcelona, Spain, 2005.

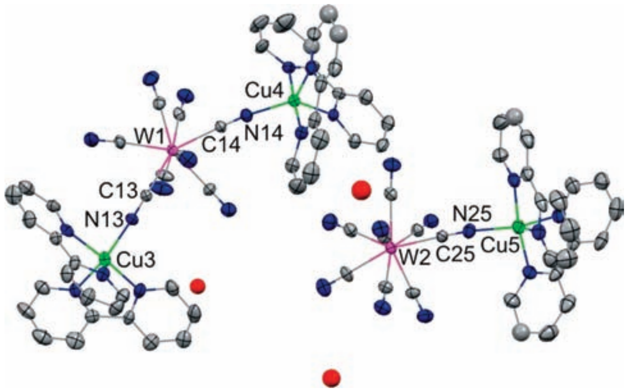

Figure 2. Structure of **2** with selected atoms labeling. Colors used: W, magenta; Cu, green; C, gray; N, blue; O, red. Thermal elipsoids of 25% probability are shown.

anions such as ClO_4^-,[55] PF_6^-,[56] SO_4^{2-},[57] $C(CN)_3^-$,[58] or $F_3CSO_3^-$[59] as well as with the complex anions of $Hg_2I_6^{2-}$,[60] $[Co(C_2H_{11}B_9)_2]^-$ (3,3′-commo-bis(1,2-dicarba-3-cobalt(III)-closo-dodecarborate),[61] or N-2-(phenyl)ethyliminodiacetato−copper[62] coordination systems.

The network of hydrogen bonds involving molecules of crystallization water and terminal cyano ligands forms the 2-D layers extending in the *bc* crystallographic plane (Figure S2, Supporting Information). The face-to-face and edge-to-face $\pi-\pi$ stacking interactions between phenanthroline ligands of $[Cu(phen)_3]^{2+}$ and $\{[Cu(phen)_2]_2[W(CN)_8]_2\}^{2-}$ ions with distances of 3.5 and 3.65 Å, respectively, co-stabilize the supermolecular 3D architecture of **1**. The space between the complex ions is filled with the perchlorate anions and crystallization water molecules. Intermetallic through-space Cu2−W1 distances are longer than 7.5 Å.

The crystal structure of **2** consists of the $[(bpy)_2Cu(\mu\text{-}NC)W(CN)_6(\mu\text{-}CN)Cu(bpy)_2]^+$ trinuclear cations, the $[(bpy)_2Cu(\mu\text{-}NC)W(CN)_7]^-$ dinuclear anions, and crystallization water molecules (Figure 2). Selected bond lengths and angles are presented in Table 3. The analysis of the ϕ and δ angles along with CShM reveals that the octacyanotungstate(V) moieties have well-defined square antiprismatic (SAPR-8) geometry with a minor dodecahedral DD-8 contribution (Tables S1 and S2 and Figure S1, Supporting Information). The W1 center forms two cyano bridges to Cu3 and Cu4 metal ions, separated by a C13−W1−C14 angle of 138.9(3)°, whereas W2 forms a single bridge to Cu5. The $[Cu(bpy)_2(NC)]$ moiety displays trigonal bipyramidal (TBPY-5) geometry with the single cyano bridge coordinated in the equatorial position. The W−CN−Cu linkages are relatively short and are characterized by Cu−N bond lengths very close to 2.0 Å, W−Cu distances close to 5.3 Å, and Cu−N−C angles above 173°. The distances between metal ions from the different cyano-bridged units are greater than 7 Å.

The H bonds between the water molecules and the terminal cyano ligands with face-to-face $\pi-\pi$ stacking interactions are shown in Figure S3 (Supporting Information). The mean distance between aromatic rings is 3.7 Å.

Magnetic Properties. The temperature dependence of $\chi T(T)$ measured at 1 kOe for **1** is presented in Figure 3. At 300 K, the χT value of 2.55(5) cm^3 K mol^{-1} is close to the 2.25 cm^3 K mol^{-1} expected for four Cu^{II} ($S = 1/2$) and two W^{V} ($S = 1/2$) ions assuming $g = 2.0$. On cooling down, the χT value increases slowly, reaching a smooth maximum around 20 K, then drops down. The magnetization measured at 2 K (Figure 4) at 50 kOe reaches 5.8 Nβ per formula unit.

The formula unit of **1** consists of the $Cu^{II}_2W^{V}_2$ tetramer and two isolated Cu^{II} ions. The magnetic data were modeled assuming that only interactions within the $Cu^{II}_2W^{V}_2$ tetramer are important, neglecting any intermolecular interaction. Due to the substantially different Cu−N bond lengths and Cu−N−C angles of the cyano bridges within the tetramer (see Table 2), two different exchange constants of isotropic Heisenberg interaction were introduced, creating a rectangle. The Hamiltonian

$$\mathbf{H_4} = -J_1(\mathbf{S_{1Cu}S_{4W}} + \mathbf{S_{3Cu}S_{2W}}) - J_2(\mathbf{S_{1Cu}S_{2W}} + \mathbf{S_{3Cu}S_{4W}}) - [g_{Cu}(S^z_{1Cu} + S^z_{3Cu}) + g_W(S^z_{2W} + S^z_{4W})]H\beta \quad (1)$$

which is a 16 × 16 matrix, was diagonalized numerically, and the magnetic moment of the tetramer was calculated as

$$M = N\sum_n (-\partial E_n/\partial H)\exp(-E_n/k_BT)/\sum_n \exp(-E_n/k_BT) \quad (2)$$

where E_n denotes eigenvalues of H_4. Such a method, contrary to the van Vleck approximation, allows us to calculate the $M(H)$ curve at low temperatures and high fields. The signal from the two remaining Cu^{II} ions was calculated separately from the Brillouin function. The parameters obtained from the fit to $\chi T(T)$ data above 6 K are $J_1 = 39(4)$ cm^{-1}, $J_2 = -1.6(4)$ cm^{-1}, and $g_{Cu} = 2.15(3)$, with the g_W value fixed to 2.00. In spite of limiting the range of fitting (to avoid a possible influence of intermolecular interactions), the data below 6 K are well reproduced; also, the calculated $M(H)$ curve at 2 K shown in Figure 4 is in reasonable agreement with the experimental data. Taking into account the possible intermolecular interaction J', we obtained the values $J_1 = 39$ cm^{-1}, $J_2 = 1.8$ cm^{-1}, and $J' = -0.3$ cm^{-1}. Thus, the value of J_1 is well estimated from the experiment independently of the theoretical model used. The definite conclusion regarding J_2 is that $|J_2| < 2$ cm^{-1}.

The temperature dependence of χT for **2** is shown in Figure 3. The χT value reaches 2.1 cm^3 K mol^{-1} at 300 K and reasonably corresponds to the expected high temperature limit of 1.88 cm^3 K mol^{-1} for five 1/2 spins with $g = 2.00$. The metric parameters of all three CN bridges are similar (Table 3), so the magnetic data were interpreted assuming

---

(55) Anderson, O. P. *J. Chem. Soc., Dalton Trans.* **1973**, 1237.
(56) Seco, J. M.; Gonzalez Garmendia, M. J.; Quiros, M. *J. Coord. Chem.* **2002**, *55*, 345.
(57) He, H.-Y.; Zhu, L.-G. *Chin. J. Inorg. Chem.* **2003**, *19*, 317.
(58) Potočnak, J.; Pohlova, M.; Wagner, C.; Jäger, L. *Acta Crystallogr., Sect. E* **2002**, *58*, m595.
(59) Sletten, J.; Julve, M. *Acta Chem. Scand.* **1999**, *53*, 631.
(60) Oh, M.-J.; Lee, Y.-M.; Lee, S. Y.; Kang, S. K.; Choi, S.-N. *Acta Crystallogr., Sect. C* **2006**, *62*, m51.
(61) Choquesillo-Lazarte, D.; Sanchez-Moreno, M. J.; Bugella-Altamirano, E.; Moyano-Gallego, M. J.; Martin-Ramos, J. D.; Gonzalez-Perez, J. M.; Carballo, R.; Niclos-Gutierrez, J. *Z. Anorg. Allg. Chem.* **2003**, *629*, 291.
(62) Polyanskaya, T. M.; Volkov, V. V.; Drozdova, M. K. *J. Struct. Chem.* **2003**, *44*, 690.

Table 3. Selected Bond Lengths [Å], Angles [deg], and Geometric Parameters of Cyano Bridges for **2**

Cu3−N31	1.973(8)	Cu4−N44	1.972(8)	Cu5−N53	1.985(9)
Cu3−N33	1.990(7)	Cu4−N41	1.981(7)	Cu5−N51	1.991(9)
Cu3−N13	2.002(7)	Cu4−N14	1.996(7)	Cu5−N25	2.017(8)
Cu3−N32	2.062(8)	Cu4−N42	2.066(7)	Cu5−N52	2.077(9)
Cu3−N34	2.090(8)	Cu4−N43	2.088(9)	Cu5−N54	2.086(9)
Cu3−N13−C13	176.2(8)	θ W1−C13	59.5	C13−W1−C14	138.9(3)
Cu4−N14−C14	173.5(7)	θ W1−C14	58.2		
Cu5−N25−C25	173.1(8)	θ W2−C25	58.3		

the same exchange interaction constant J for all pairs of spins. To reproduce a maximum observed experimentally in χT around 10 K, it was necessary to introduce an effective intermolecular interaction. In the crystal structure of **2**, each Cu_2W unit has four Cu_2W and four CuW units, and each CuW unit also has four Cu_2W and four CuW units in their neighborhood. To calculate the magnetic moment M for high fields, it was necessary to solve numerically the full molecular field equation

$$M = M_2(M\lambda + H) + M_3(M\lambda + \mathrm{H}) \tag{3}$$

where $M_2(H,T)$ and $M_3(H,T)$ denote the magnetic moment of the dinuclear and the trinuclear units, respectively, which were calculated from full Hamiltonians without the van Vleck approximation. In the linear approximation, the equations simplify to a form similar to that for the classical, single sublattice network, and the susceptibility can be calculated as $\chi = (\chi_2 + \chi_3)/(1 - \lambda(\chi_2 + \chi_3))$, where $\lambda = 4J'k_B/(Ng_{avg}{}^2\beta^2)$ and χ_2 and χ_3 are the susceptibilities of the isolated CuW unit and Cu_2W, respectively. The values obtained from the fit to the $\chi T(T)$ data are J = 35(7) cm^{-1}, $4J'$ = −0.30(8) cm^{-1}, and g_{Cu}=2.15(5). The g_W value was fixed equal to 2.00. The calculated $M(H, T = 2$ K) curve is in reasonable agreement with the experimental data.

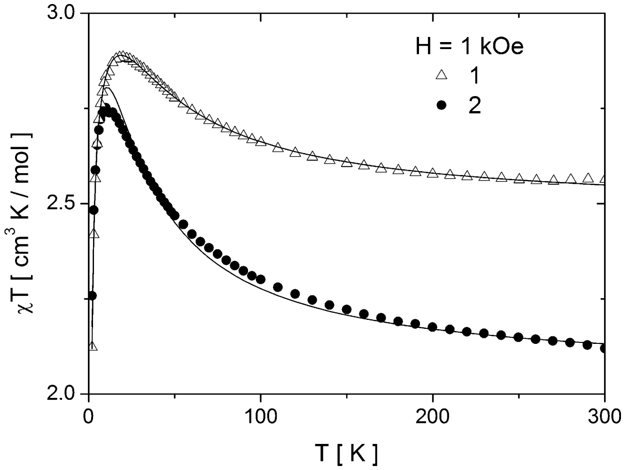

Figure 3. Thermal dependence of χT for **1** (triangles) and **2** (cirlces) with their respective fitted curves (solid lines).

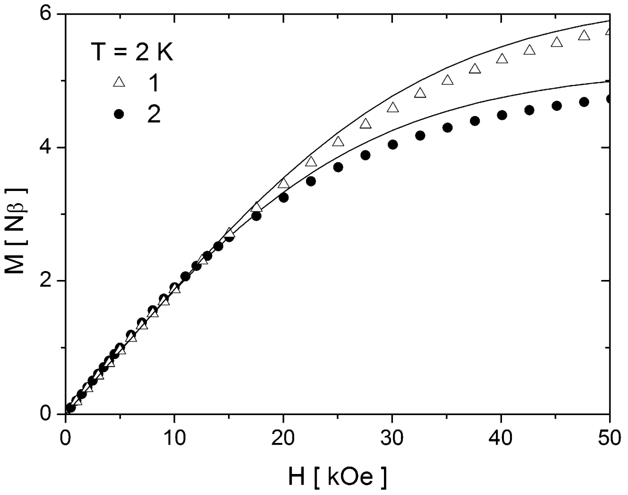

Figure 4. Field-dependent magnetization $M(H)$ for **1** (triangles) and **2** (cirlces) with their respective fitted curves (solid lines).

DFT Calculations. Calculations of J have been realized using DFT methods as described in the computational methodology section. The calculations have been performed on the whole molecule, without any modification for the ligand, and with two, three, and four metal atoms for the dinuclear, trinuclear, and tetranuclear subunits, respectively. The calculated J values are +39.6 cm^{-1} for dinuclear, +22.4 cm^{-1} for trinuclear, and +13.2 cm^{-1} for tetranuclear moieties. For the tetranuclear unit present in **1**, the experimental magnetic data have been fitted using two different J values, J_1 = +39 cm^{-1} and J_2 = −1.6 cm^{-1}, while the DFT calculations give the J_{av} = +13.2 cm^{-1}. The magnetic properties of compound **2** consisting of the dinuclear and trinuclear units have been characterized by the single value of J = +35 cm^{-1}, while the mean calculated J_{av} value for **2** is +31.0 cm^{-1}. The DFT calculations confirm the domination of W−CN−Cu ferromagnetic interaction, which can be rationalized in terms of the natural magnetic orbitals (Figure 6). The "magnetic natural orbitals" are defined as the natural orbitals of the high-spin state (S = 1) with occupancy very close to 1. The molecular orbital of the $[W(CN)_8]^{3-}$ moiety involves the metal-centered d_{z^2} orbital and the π orbitals of the CN ligands. On the Cu side, the molecular orbital results from the mixing of the σ system of the ligands (i.e., the two bidentate ligands and the N atom of the bridging cyanide) with the d_{z^2} orbital of the Cu ion. The ferromagnetic interaction is rationalized by taking advantage of the Kahn's model,[48] where the exchange parameter J is expressed as the sum of two terms of opposite sign: $J = J_F + J_{AF}$, with $J_F = 2k > 0$ and $J_{AF} = 4\beta s < 0$. In this model, k denotes the bielectronic exchange integral, β is the monoelectronic

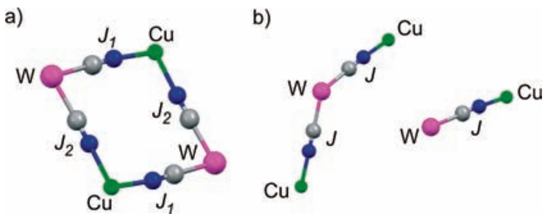

Figure 5. The exchange interactions within the cyano-bridged molecular assemblies in **1** (a) and **2** (b) represented by (J_1, J_2) and J parameters, respectively.

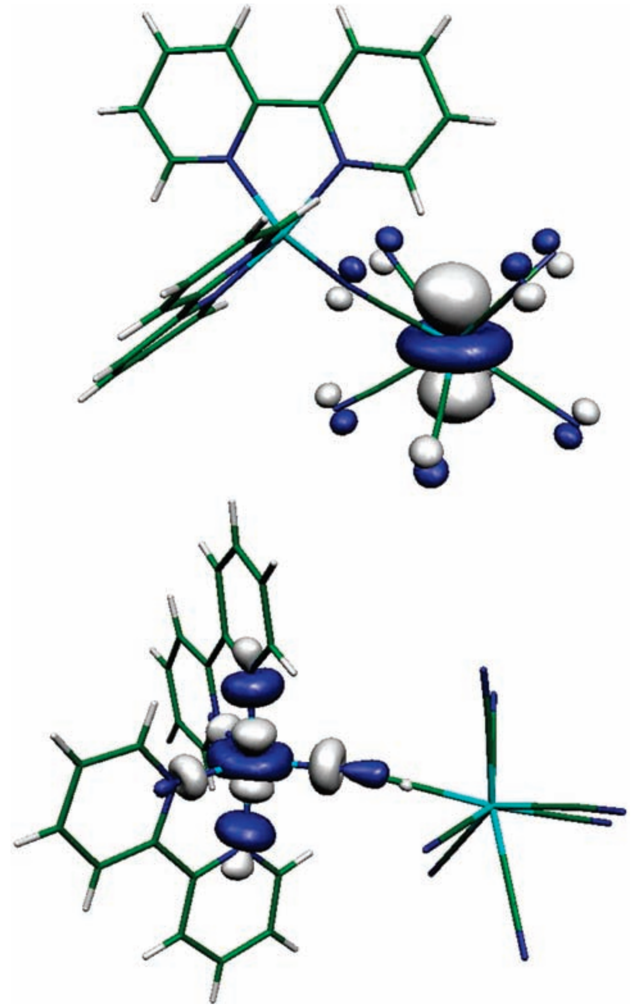

Figure 6. Magnetic natural orbitals of the Cu−NC−W linkage (high spin state). One orbital is mainly localized on the W atom (top), and the other is mainly localized on the Cu atom (bottom).

resonance integral, and s stands for the monoelectronic overlap integral. This expression is valid when two centers, each bearing one unpaired electron, are coupled. When localized molecular orbitals have a very small overlap (i.e., $s \approx 0$), the interaction between the two metal atom spin carriers is expected to be ferromagnetic. Being delocalized in different types of systems (π on the W side and σ on the Cu side), the overlap s is expected to be small and the interaction between W and Cu is expected to be ferromagnetic.

Spin density for the ground ferromagnetic state of the W^{V}−CN−Cu^{II} linkage characteristic for **1** and **2** is shown in Figure 7. The spin density of the octacyanotungstate is localized in the π system of the terminal cyano ligands, revealing postive values on the N atoms and negative values on the C donors, due to spin polarization. In the case of the Cu center, some spin density is delocalized in the σ system of the surrounding atoms, as expected from classical ligand field theory.

The J values calculated by DFT decrease from the dinuclear to the trinuclear and finally to the tetranuclear subunits, which can be rationalized in terms of the bending angle of the Cu−NC linkage and the square-antiprismatic structure of the $[W(CN)_8]^{3-}$ ion, although quite distorted in the case of the tetranuclear moiety. It has been previously shown in the Cr^{III}−CN−Ni^{II} systems that the J value depends strongly on the CN−Ni^{II} bending angle.[63] The value of J was found to vary linearly with this angle, the strongest ferromagnetic interactions being anticipated for a 180° angle. An overall antiferromagnetic behavior between Cr and Ni is predicted for angles lower than 145°. Remembering that the t_{2g} unpaired electrons of Cr^{III} delocalize in the π system and the e_g electron of Ni^{II} delocalizes in the σ system, this decrease in J can be explained in terms of overlap of the σ and π systems. A bending of the bridging ligand tends to decrease the symmetry of the system, allowing the overlap of the σ and π systems. The more the system deviates from linearity, the more this overlap is pronounced and, according to the Kahn's model, the more the antiferromagnetic component J_{AF} is important. In the three subunits studied, the angles CN−Cu^{II} are respectively 173.1° for the dinuclear, 173.4° and 176.1° for the trinuclear, and 169.4 and 154.7° for the tetranuclear unit. A particularly small CN−Cu^{II} angle is observed in the case of the tetranuclear unit, justifying the small antiferromagnetic interaction J_2 that is observed.

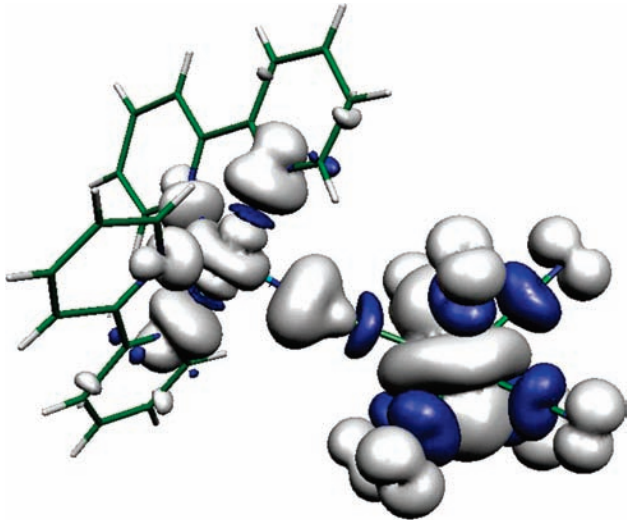

Figure 7. Spin density of the high spin state for the Cu−NC−W linkage. Positive spin density shown in gray and negative in blue.

Conclusions

The finite size and the low nuclearity of **1** and **2** allowed application of the simple theoretical model of reliable calculation of the magnitude of intermetallic W(V)−Cu(II) coupling. The important characteristic of the M^{V}−CN−Cu^{II} linkage is the pronounced domination of the strong ferromagnetic W^{V}−CN−Cu^{II} coupling for the equatorially coordinated cyano bridges at Cu(II) centers with the coupling constants for the reference compounds displaying values in the range of 30−40 cm^{-1} (Table S4, Supporting Information). In the case of axial cyano bridges, the antiferromagnetic contribution is dominating, which leads to a lowering of J below 6 cm^{-1} and, in some cases, to small negative values.

---

[63] Marvaud, V.; Herrera, J.-M.; Barilero, T.; Tuyeras, F.; Garde, R.; Sciuller, A.; Decroix, C.; Cantuel, M.; Desplanches, C. *Monatsh. Chem.* **2003**, *134*, 149–163.

The magnetic properties of **1** and **2** and the correlation of the J_{CuW} parameters with the geometry of cyano bridges at copper(II) centers are based on the DFT calculations confirming the experimental results. The DFT calculations reveal the small overlapping between the natural magnetic orbitals of the copper(II) and tungsten(V) centers. Therefore, the design of bimetallic cyano-bridged $\mathrm{Cu^{II}[M^{V}(CN)_8]}$ compounds with strong ferromagnetic magnetic interaction requires the use of preprogrammed copper(II) precursors, enabling exclusively equatorial coordination of the $\mathrm{CN^-}$ bridges. The control of the geometric parameters is important: the almost linear Cu−N−C angles favor ferromagnetic $\mathrm{M^{V}{-}CN{-}Cu^{II}}$ interaction, and the short $\mathrm{Cu{-}N_{CN}}$ distances facilitate the magnetic contact between the metallic centers. The rational design and construction of the new zero-dimensional architectures should allow more elaborate magnetostructural correlation and tuning of the magnetic properties. Studies along this line are currently in progress.

Acknowledgment. This work was partially supported by the European Grant NoE “MAGMANet” (NMP3-CT-2005-515767).

Supporting Information Available: CIF files for **1** and **2**; values of the shape-determining parameters for $\mathrm{[W(CN)_8]^{3-}}$ polyhedra in **1** and **2**; correlation of J coupling constant with cyano bridge position in the coordination sphere of copper in Cu−M (M = Mo, W) assemblies; figures of noncovalent interactions stabilizing 3D architectures of **1** and **2**. This material is available free of charge via the Internet at http://pubs.acs.org.

IC801989B